ORIGINAL PAPER

SORET AND DUFOUR EFFECTS ON UNSTEADY HYDROMAGNETIC FREE CONVECTIVE FLUID FLOW PAST AN INFINITE VERTICAL POROUS PLATE IN THE PRESENCE OF CHEMICAL REACTION

N.V.N BABU[1], AJIT PAUL[2], MURALI G[3]

Manuscript received: 02.02.2015; Accepted paper: 07.03.2015;

Published online: 30.03.2015.

Abstract. *In this research paper, the numerical solutions are carried out for the combined effects of Soret and Dufour on unsteady hydromagnetic free convective flow of a Newtonian, viscous, electrically conducting fluid on a continuously vertical permeable surface in the presence of heat source, a first – order homogeneous chemical reaction and the mass flux are reported. The plate is assumed to move with a constant velocity in the direction of fluid flow. A uniform magnetic field acts perpendicular to the porous surface, which absorbs the fluid with a suction velocity varying with time. The dimensionless governing equations for this investigation are solved numerically by finite difference method using symbolic software MATLAB. Graphical results for velocity, temperature and concentration profiles of both phases based on the numerical solutions are presented and discussed.*

Keywords: *Soret and Dufour, Chemical reaction, MHD, Porous medium and Finite difference method.*

1. INTRODUCTION

The Soret and Dufour effects have garnered considerable interest in both Newtonian and non – Newtonian convective heat and mass transfer. Such effects are significant when density differences exist in the flow regime. Soret and Dufour effects are important for intermediate molecular weight gases in coupled heat and mass transfer in binary systems, often encountered in chemical process engineering and also in high – speed aerodynamics. Soret and Dufour effects are also critical in various porous flow regimes occurring in chemical and geophysical systems. There are few studies about the Soret and Dufour effects in a Darcy or non – Darcy porous medium. Anghel et al. [1] have examined the composite Soret and Dufour effects on free convective heat and mass transfer in a Darcian porous medium with Soret and Dufour effects. Emmunuel et al. [2] have discussed Thermal – diffusion and diffusion – thermo effects on combined heat and mass transfer of a steady MHD convective and slip flow due to a rotating disk with viscous dissipation and Ohmic heating. Another contribution to the theme of Dufour and Soret effects can be found in the paper by Afify [3], where there is a non – Darcy free convection past a vertical surface with temperature viscosity. Lakshmi Narayana and Murthy [4] studied the Soret and Dufour effects on free convection heat and mass transfer from a horizontal flat plate in a Darcy porous medium. Postelnicu [5] studied the influence of chemical reaction along with Soret and

[1] S.V.E.R.I Engineering College, Department of Mathematics, Pandharpur, India. E-mail: nvnb45@gmail.com.
[2] SHIATS University, Department of Mathematics, Allahabad, India.
[3] GITAM University, Department of Mathematics, Rudraram, India.

Dufour effects in the absence of magnetic field on free convection. El – Arabawy [6] studied the Soret and Dufour effects in a vertical plate with variable surface temperature. Postelnicu [7] analyzed the effect of Soret and Dufour on heat and mass transfer at a stagnation point. Tak et al. [8] investigated the MHD free convection radiation in the presence of Soret and Dufour.

Combined heat and mass transfer problems with chemical reaction are of importance in many processes and have, therefore, received a considerable amount of attention in recent years. In processes such as drying, evaporation at the surface of a water body, energy transfer in a wet cooling tower and the flow in a desert cooler, heat and mass transfer occur simultaneously. Natural or free convection processes in double diffusive convection are also encountered in many natural processes, such as evaporation, condensation and agricultural drying, and in many industrial applications, such as the curing of plastics, cleaning and chemical processing of materials relevant to the manufacture of printed circuitry. Many practical diffusive operations involve the molecular diffusion of a species in the presence of chemical reaction within or at the boundary. Therefore, the study of heat and mass transfer with chemical reaction is of great practical importance to engineers and scientists. In light of these various applications, Analytical solutions for heat and mass transfer by laminar flow of a Newtonian, viscous, electrically conducting and heat generation or absorbing fluid on a continuously vertical permeable surface in the presence of a radiation, a first – order homogeneous chemical reaction and the mass flux are reported by Kesavaiah et al. [9]. The plate is assumed to move with a constant velocity in the direction of fluid flow. A uniform magnetic field acts perpendicular to the porous surface, which absorbs the fluid with a suction velocity varying with time. The dimensionless governing equations for this investigation are solved analytically using two – term harmonic and non – harmonic functions. Seddeek et al. [10] studied the effects of chemical reaction and variable viscosity on hydromagnetic mixed convection heat and mass transfer through porous media. Das et al. [11] studied the effects of mass transfer on flow past an impulsively started infinite vertical plate with constant heat flux and chemical reaction. Effects of chemical reaction heat and mass transfer on laminar flow along a semi – infinite horizontal plate have been studied by Anjalidevi and Kandasamy [12]. Takhar et al. [13] analyzed the convective flow and mass transfer on a stretching sheet with a magnetic field and chemically reactive species. Muthucumaraswamy [14] investigated the effects of suction on heat and mass transfer along a moving vertical surface in the presence of chemical reaction. Afify [15] analyzed MHD free convective flow and mass transfer over a stretching sheet with chemical reaction. Raptis and Perdikis [16] studied viscous flow over a non – linearly stretching sheet in the presence of a chemical reaction and magnetic field. Postelnicu [17] studied the influence of nth order chemical reaction on heat and mass transfer by natural convection from vertical surfaces in porous media considering Soret and Dufour effects. The effect of variable viscosity and thermal conductivity on mixed convection flow and heat transfer along a semi – infinite non – linear stretching sheet embedded in a saturated porous medium in the presence of viscous dissipation, Soret and Dufour, thermal radiation, non – uniform heat source/sink and first order chemical reaction studied by Dulal Pal and Hiranmoy Mondal [18]. Dulal Pal and Hiranmoy Mondal [19] deal with the thermophoresis particle deposition and Soret – Dufour effects on the convective flow, heat and mass transfer characteristics of an incompressible Newtonian electrically conducting fluid having temperature dependent viscosity over a non – isothermal wedge in the presence of thermal radiation. Ching – Yang Cheng [20] studied the heat and mass transfer characteristics of natural convection near a vertical wavy cone in a fluid saturated porous medium with Soret and Dufour effects. The surface of the wavy cone is kept at constant temperature and concentration. The governing equations are transformed into a set of coupled differential equations, and the obtained boundary layer equations are solved by the cubic spline collocation method. Combined effects of Soret(thermal – diffusion) and Dufour (diffusion – thermo) on mixed convection over a stretching sheet embedded in a saturated porous medium in the presence of thermal radiation and first order chemical reaction are studied by Dulal Pal and Hiranmoy Mondal [21]. The effects of thermal radiation and Heat source on an unsteady MHD free convection flow past an infinite vertical plate with thermal – diffusion and diffusion – thermo discussed by Srinivasa Raju et al. [22]. A numerical model is developed by Dulal Pal and Sewli Chatterjee [23] to study the MHD mixed convection with the combined action of Soret and Dufour on heat and mass transfer of a power – law fluid over an inclined plate in a porous medium in the presence of variable thermal conductivity, thermal radiation, chemical reaction and Ohmic dissipation and suction/injection.

Hence, the main objective of the present investigation is to study the combined effects of Soret and Dufour on unsteady hydromagnetic free convective flow of a Newtonian, viscous, electrically conducting fluid on a continuously fluid past a vertical porous plate subjected to variable suction in presence of radiation absorption, mass diffusion, chemical reaction and heat source parameter of heat generating It is assumed that the plate is embedded in a uniform porous medium and moves with a constant velocity in the flow direction in the presence of a transverse magnetic field. It is also assumed that temperature over which are superimposed an exponentially varying with time. The equations of continuity, linear momentum, energy and diffusion, which govern the flow field, are solved numerically by using finite difference method which is more economical from computational view point. The behavior of the velocity, temperature, concentration, skin – friction, Nusselt number and Sherwood number has been discussed for variations in the governing parameters.

2. MATHEMATICAL FORMULATION

We consider unsteady flow of a laminar, viscous, electrically conducting fluid past a semi – infinite vertical permeable moving plate embedded in a uniform porous medium and subjected to a uniform transverse magnetic field in the presence of thermal and concentration buoyancy effects. We made the following assumptions. In cartesian coordinate system, let $x'-$axis is taken to be along the plate and the $y'-$axis normal to the plate. Since the plate is considered infinite in $x'-$direction, hence all physical quantities will be independent of $x'-$direction. The wall is maintained at constant temperature (T'_w) and concentration (C'_w) higher than the ambient temperature (T'_∞) and concentration (C'_∞) respectively. A uniform magnetic field of magnitude B_o is applied normal to the plate. The transverse applied magnetic field and magnetic Reynold's number are assumed to be very small, so that the induced magnetic field is negligible. The fluid properties are assumed to be constant except that the influence of density variation with temperature has been considered only in the body – force term. The chemical reactions are taking place in the flow and all thermophysical properties are assumed to be constant of the linear momentum equation which is approximated according to the Boussinesq's approximation. Due to the semi – infinite plane surface assumption, the flow variables are functions of y' and the time t' only. It is assumed that there is no applied voltage which implies the absence of an electric field. The fluid has constant kinematic viscosity and constant thermal conductivity, and the Boussinesq approximation have been adopted for the flow. At time $t' > 0$ the plate is given an impulsive motion in the direction of flow i.e. along $x'-$axis against the gravity with constant velocity U_o. In addition, it is assumed that the temperature and the concentration at the wall as well as

the suction velocity are exponentially varying with time. Under these assumptions, the equations that describe the physical situation are given by
Equation of Continuity:

$$\frac{\partial v'}{\partial y'} = 0 \tag{1}$$

Momentum Equation:

$$\frac{\partial u'}{\partial t'} + v'\frac{\partial u'}{\partial y'} = \nu\frac{\partial^2 u'}{\partial y'^2} + g\beta\left(T' - T'_\infty\right) + g\beta^*\left(C' - C'_\infty\right) - \left(\frac{\sigma B_o^2}{\rho} + \frac{\nu}{K'}\right)u' \tag{2}$$

Energy Equation:

$$\frac{\partial T'}{\partial t'} + v'\frac{\partial T'}{\partial y'} = \frac{1}{\rho C_p}\left[\kappa\frac{\partial^2 T'}{\partial y'^2} + Q_o\left(T' - T'_\infty\right)\right] + \frac{D_m k_T}{C_S C_P}\frac{\partial^2 C'}{\partial y'^2} \tag{3}$$

Species Diffusion Equation:

$$\frac{\partial C'}{\partial t'} + v'\frac{\partial C'}{\partial y'} = D\frac{\partial^2 C'}{\partial y'^2} - K'_r\left(C' - C'_\infty\right) + \frac{D_m k_T}{T_m}\frac{\partial^2 T'}{\partial y'^2} \tag{4}$$

The third and fourth terms on the right hand side of equation (2) denote the thermal and concentration buoyancy effects respectively. Also the last term on the right hand side of the energy equation (3) represents the radiative heat flux term. It is assumed that the permeable plate moves with a constant velocity in the direction of fluid flow, and the free stream velocity follows the exponentially increasing small perturbation law.

With the following initial and boundary conditions:

$$\left.\begin{array}{l} t' \le 0 : u' = 0,\ T' = T'_\infty,\ C' = C'_\infty \quad for \quad all \quad y' \\ t' > 0 : \left\{\begin{array}{l} u' = u'_p,\ T' = T'_\infty + \varepsilon\left(T'_w - T'_\infty\right)e^{n't'},\ C' = C'_\infty + \varepsilon\left(C'_w - C'_\infty\right)e^{n't'} \quad at \quad y' = 0 \\ u' \to 0,\ T' \to 0,\ C' \to 0 \quad as \quad y' \to \infty \end{array}\right. \end{array}\right\} \tag{5}$$

From equation (1), it is clear that the suction velocity at the plate is either a constant or a function of time. Hence the suction velocity normal to the plate is assumed in the form

$$v' = -V_o\left(1 + \varepsilon A e^{n't'}\right) \tag{6}$$

where A is a real positive constant, ε and εA is small values less than unity, and V_o is scale of suction velocity which is non – zero positive constant. The negative sign indicates that the suction is towards the plate. In order to write the governing equations and the boundary conditions in dimensionless from, the following non – dimensional quantities are introduced.

$$\left.\begin{array}{l} y=\dfrac{y'V_o}{\nu},\ t=\dfrac{t'V_o^2}{\nu},\ u=\dfrac{u'}{U_o},\ v=\dfrac{v'}{V_o^2},\ \theta=\dfrac{T'-T'_\infty}{T'_w-T'_\infty},\ \phi=\dfrac{C'-C'_\infty}{C'_w-C'_\infty},\ n=\dfrac{n'\nu}{V_o^2},\ U_p=\dfrac{u'_p}{U_o}, \\ M=\left(\dfrac{\sigma B_o^2}{\rho}\right)\dfrac{\nu}{V_o^2},\ Gr=\dfrac{g\beta\nu\left(T'_w-T'_\infty\right)}{U_oV_o^2},\ Gc=\dfrac{g\beta^*\nu\left(C'_w-C'_\infty\right)}{U_oV_o^2},\ \Pr=\dfrac{\nu\rho C_p}{\kappa}=\dfrac{\nu}{\alpha},\ Sc=\dfrac{\nu}{D}, \\ Sr=\dfrac{D_mk_T(T'_w-T'_\infty)}{\nu T_m(C'_w-C'_\infty)},\ K=\dfrac{K'V_o^2}{\nu^2},\ S=\dfrac{\nu Q_o}{\rho C_pV_o^2},\ k_r=\dfrac{K'_r\nu}{V_o^2},\ Du=\dfrac{D_mk_T(C'_w-C'_\infty)}{C_SC_P(T'_w-T'_\infty)}, \end{array}\right\} \tag{7}$$

In view of equations (6) and (7), equations (2) to (4) reduce to the following dimensional form:

$$\frac{\partial u}{\partial t}-\left(1+\varepsilon Ae^{nt}\right)\frac{\partial u}{\partial y}=\frac{\partial^2 u}{\partial y^2}-(M+\frac{1}{K})u+\left(Gr\right)\theta+\left(Gc\right)\phi \tag{8}$$

$$\frac{\partial \theta}{\partial t}-\left(1+\varepsilon Ae^{nt}\right)\frac{\partial \theta}{\partial y}=\frac{1}{\Pr}\frac{\partial^2 \theta}{\partial y^2}+S\theta+\left(Du\right)\left(\frac{\partial^2 \phi}{\partial y^2}\right) \tag{9}$$

$$\frac{\partial \phi}{\partial t}-\left(1+\varepsilon Ae^{nt}\right)\frac{\partial \phi}{\partial y}=\frac{1}{Sc}\frac{\partial^2 \phi}{\partial y^2}-\left(k_r\right)\phi+\left(Sr\right)\left(\frac{\partial^2 \theta}{\partial y^2}\right) \tag{10}$$

The corresponding initial and boundary conditions in dimensionless form are:

$$\left.\begin{array}{l} t\le 0:\ u=0,\ \theta=0,\ \phi=0\ \ for\ \ all\ \ y \\ t>0:\begin{cases} u=U_p,\ \theta=1+\varepsilon e^{nt},\ \phi=1+\varepsilon e^{nt}\ \ at\ \ y=0 \\ u\to 0,\ \theta\to 0,\ \phi\to 0\ \ as\ \ y\to\infty \end{cases} \end{array}\right\} \tag{11}$$

All the physical parameters are defined in the nomenclature. It is now important to calculate the physical quantities of primary interest, which are the local wall shear stress, the local surface heat and mass flux. Given the velocity field in the boundary layer, we can now calculate the local wall shear stress (i.e., skin – friction) is given by and in dimensionless form, we obtain knowing the temperature field, it is interesting to study the effect of the free convection and radiation on the rate of heat transfer. This is given by which is written in dimensionless form as

$$\tau=\frac{\tau_w}{\rho u_w^2},\ \tau_w=\left[\mu\frac{\partial u}{\partial y}\right]_{y'=0}=\rho V_o^2u'(0)=\left[\frac{\partial u}{\partial y}\right]_{y=0} \tag{12}$$

The dimensionless local surface heat flux (i.e., Nusselt number) is obtained as

$$N_u(x')=-\left[\frac{x'}{(T'_w-T'_\infty)}\frac{\partial T'}{\partial y'}\right]_{y'=0}\quad \text{then}\ \ Nu=\frac{N_u(x')}{R_{e_x}}=-\left[\frac{\partial \theta}{\partial y}\right]_{y=0} \tag{13}$$

The definition of the local mass flux and the local Sherwood number are respectively given by with the help of these equations, one can write

$$S_h(x') = -\left[\frac{x'}{(C'_w - C'_\infty)}\frac{\partial C'}{\partial y'}\right]_{y'=0} \text{ then } Sh = \frac{S_h(x')}{R_{e_x}} = -\left[\frac{\partial \phi}{\partial y}\right]_{y=0} \tag{14}$$

where $R_{e_x} = -\frac{V_o x'}{\nu}$ is the Reynold's number.

3. METHOD OF SOLUTION

We shall solve the system of partial differential equations numerically using the finite difference technique and equations (8) – (10) yield.

$$\left(\frac{u_i^{j+1} - u_i^j}{\Delta t}\right) - B\left(\frac{u_{i+1}^j - u_i^j}{\Delta y}\right) = \left(\frac{u_{i+1}^j - 2u_i^j + u_{i-1}^j}{(\Delta y)^2}\right) - \left(M + \frac{1}{K}\right)u_i^j + (Gr)\theta_i^j + (Gc)\phi_i^j \tag{15}$$

$$\left(\frac{\theta_i^{j+1} - \theta_i^j}{\Delta t}\right) - B\left(\frac{\theta_{i+1}^j - \theta_i^j}{\Delta y}\right) = \frac{1}{\Pr}\left(\frac{\theta_{i+1}^j - 2\theta_i^j + \theta_{i-1}^j}{(\Delta y)^2}\right) + S\theta_i^j + (Du)\left(\frac{\phi_{i+1}^j - 2\phi_i^j + \phi_{i-1}^j}{(\Delta y)^2}\right) \tag{16}$$

$$\left(\frac{\phi_i^{j+1} - \phi_i^j}{\Delta t}\right) - B\left(\frac{\phi_{i+1}^j - \phi_i^j}{\Delta y}\right) = \frac{1}{Sc}\left(\frac{\phi_{i+1}^j - 2\phi_i^j + \phi_{i-1}^j}{(\Delta y)^2}\right) - (k_r)\phi_i^j + (Sr)\left(\frac{\theta_{i+1}^j - 2\theta_i^j + \theta_{i-1}^j}{(\Delta y)^2}\right) \tag{17}$$

where $B = 1 + \varepsilon A e^{nt}$, the indices i and j refer to y and t respectively.

The initial and boundary conditions (15) yield.

$$\left.\begin{array}{l} t \le 0: \{u_i^j = 0,\ \theta_i^j = 0,\ \phi_i^j = 0 \quad for\ all\ y \\ t > 0: \begin{cases} u_i^j = U_p,\ \theta_i^j = 1 + \varepsilon e^{nt},\ \phi_i^j = 1 + \varepsilon e^{nt}\ \ at\ \ y = 0 \\ u_i^j \to 0,\ \theta_i^j \to 0,\ \phi_i^j \to 0\ \ as\ \ y \to \infty \end{cases} \end{array}\right\} \tag{18}$$

The term consistency applied to a finite difference procedure means that the procedure may in fact approximate the solution of the partial differential equation under study and not the solution of any other partial differential equation. The consistency is measured in terms of the difference between a differential equation and a difference equation. Here, we can write

$$\frac{\partial u}{\partial t} = \frac{u_i^{j+1} - u_i^j}{\Delta t} + O(\Delta t),\ \frac{\partial \theta}{\partial t} = \frac{\theta_i^{j+1} - \theta_i^j}{\Delta t} + O(\Delta t),\ \frac{\partial \phi}{\partial t} = \frac{\phi_i^{j+1} - \phi_i^j}{\Delta t} + O(\Delta t),$$

$$\frac{\partial u}{\partial y} = \frac{u_{i+1}^j - u_i^j}{\Delta y} + O(\Delta y),$$

$$\frac{\partial \theta}{\partial y} = \frac{\theta_{i+1}^j - \theta_i^j}{\Delta y} + O(\Delta y),\ \frac{\partial \phi}{\partial y} = \frac{\phi_{i+1}^j - \phi_i^j}{\Delta y} + O(\Delta y),\ \frac{\partial^2 u}{\partial y^2} = \frac{u_{i+1}^j - 2u_i^j + u_{i-1}^j}{(\Delta y)^2} + O(\Delta y)^2,$$

$$\frac{\partial^2\theta}{\partial y^2}=\frac{\theta_{i+1}^{j}-2\theta_i^{j}+\theta_{i-1}^{j}}{(\Delta y)^2}+O(\Delta y)^2 \text{ and } \frac{\partial^2\phi}{\partial y^2}=\frac{\phi_{i+1}^{j}-2\phi_i^{j}+\phi_{i-1}^{j}}{(\Delta y)^2}+O(\Delta y)^2$$

For consistency of equation (15), we estimate

$$\begin{aligned}&\left\{\left(\frac{u_i^{j+1}-u_i^{j}}{\Delta t}\right)-B\left(\frac{u_{i+1}^{j}-u_i^{j}}{\Delta y}\right)-\left(\frac{u_{i+1}^{j}-2u_i^{j}+u_{i-1}^{j}}{(\Delta y)^2}\right)+\left(M+\frac{1}{K}\right)u_i^{j}-(Gr)\theta_i^{j}-(Gc)\phi_i^{j}\right\}\\&-\left\{\frac{\partial u}{\partial t}-\left(1+\varepsilon Ae^{nt}\right)\frac{\partial u}{\partial y}-\frac{\partial^2 u}{\partial y^2}+(M+\frac{1}{K})u-(Gr)\theta-(Gc)\phi\right\}_{i,\,j}=O(\Delta t)+O(\Delta y)\end{aligned} \tag{19}$$

For consistency of equation (16), we estimate

$$\begin{aligned}&\left\{\left(\frac{\theta_i^{j+1}-\theta_i^{j}}{\Delta t}\right)-B\left(\frac{\theta_{i+1}^{j}-\theta_i^{j}}{\Delta y}\right)-\frac{1}{\Pr}\left(\frac{\theta_{i+1}^{j}-2\theta_i^{j}+\theta_{i-1}^{j}}{(\Delta y)^2}\right)-S\theta_i^{j}-(Du)\left(\frac{\phi_{i+1}^{j}-2\phi_i^{j}+\phi_{i-1}^{j}}{(\Delta y)^2}\right)\right\}\\&-\left\{\frac{\partial\theta}{\partial t}-\left(1+\varepsilon Ae^{nt}\right)\frac{\partial\theta}{\partial y}-\frac{1}{\Pr}\frac{\partial^2\theta}{\partial y^2}-S\theta-(Du)\left(\frac{\partial^2\phi}{\partial y^2}\right)\right\}_{i,\,j}=O(\Delta t)+O(\Delta y)\end{aligned} \tag{20}$$

Similarly with respect to equation (17)

$$\begin{aligned}&\left\{\left(\frac{\phi_i^{j+1}-\phi_i^{j}}{\Delta t}\right)-B\left(\frac{\phi_{i+1}^{j}-\phi_i^{j}}{\Delta y}\right)-\frac{1}{Sc}\left(\frac{\phi_{i+1}^{j}-2\phi_i^{j}+\phi_{i-1}^{j}}{(\Delta y)^2}\right)+(k_r)\phi_i^{j}-(Sr)\left(\frac{\theta_{i+1}^{j}-2\theta_i^{j}+\theta_{i-1}^{j}}{(\Delta y)^2}\right)\right\}\\&-\left\{\frac{\partial\phi}{\partial t}-\left(1+\varepsilon Ae^{nt}\right)\frac{\partial\phi}{\partial y}-\frac{1}{Sc}\frac{\partial^2\phi}{\partial y^2}+(k_r)\phi-(Sr)\left(\frac{\partial^2\theta}{\partial y^2}\right)\right\}_{i,\,j}=O(\Delta t)+O(\Delta y)\end{aligned} \tag{21}$$

Here, the right hand side of equations (19) – (21) represents truncation error as $\Delta t\to 0$ with $\Delta y\to 0$, the truncation error tends to zero. Hence our explicit scheme is consistent. Here Δy, Δt are mesh sizes along y and time direction respectively. The infinity taken as $i=1$ to n and the equations (19), (20) and (21) are solved under the boundary conditions (18), following the tri diagonal system of equations are obtained.

$$A_i X_i = B_i \ (i=1 \text{ to } n) \tag{22}$$

where A_i is the tri diagonal matrix of order $n\times n$ and X_i, B_i are the column matrices having n components. The above system of equations has been solved by Thomas Algorithm (Gauss elimination method), for velocity, temperature and concentration. In order to prove the convergence of the finite difference scheme, the computations are carried out for different values of Δt. But the Crank – Nicholson method is unconditionally stable. By changing the value of Δt there is no change in the study state condition. So, the finite difference scheme is convergent and stable.

4. RESULTS AND DISCUSSION

Numerical evaluation for the analytical solutions of this problem is performed and the results are illustrated graphically in figs. 1-17 to show the interesting features of some important significant physical parameters on the fluid and dust particle velocity. Throughout the computations we employed 0.5, 1.0, 0.1 and 0.02 and while M, K, Sr, Du, S, k_r and U_p and are varied over a range, which are listed in the figure legends. The effect of Hartmann number on velocity profiles in the boundary layer is depicted in fig. 1. From this figure it is seen that the velocity starts from minimum value at the surface and increase till it attains the peak value and then starts decreasing until it reaches to the minimum value at the end of the boundary layer for all the values of Hartmann number. It is interesting to note that the effect of magnetic field is to decrease the value of the velocity profiles throughout the boundary layer. The effect of magnetic field is more prominent at the point of peak value i.e. the peak value drastically decreases with increases in the value of magnetic field, because the presence of magnetic field in an electrically conducting fluid introduce a force called the Lorentz force, which acts against the flow if the magnetic field is applied in the normal direction, as in the present problem. This type of resisting force slows down the fluid velocity as shown in this figure.

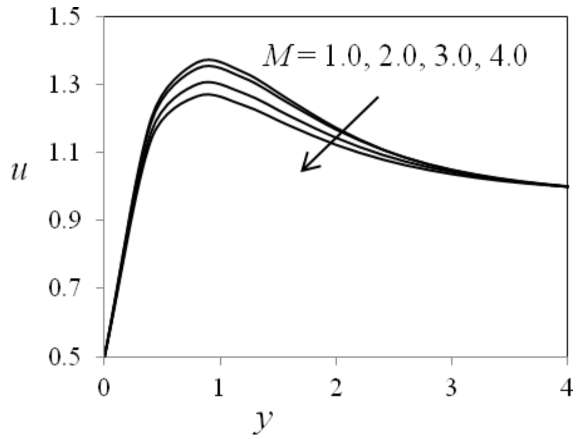

Figure 1. Velocity profiles for different values of Hartmann number

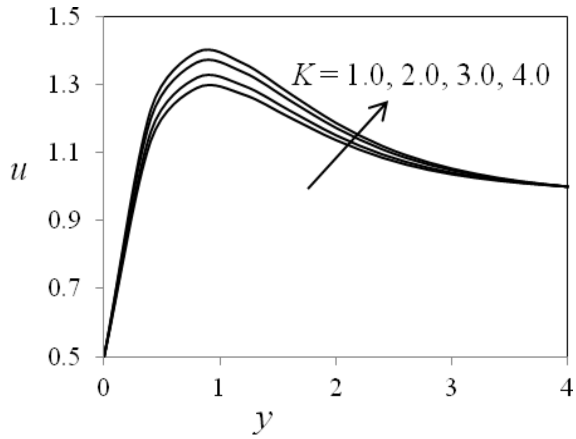

Figure 2. Velocity profiles for different values of Permeability parameter

Fig. 2 shows the velocity profiles for different values of the permeability parameter, clearly as increases the peak values of the velocity tends to increase. The effect of increasing the value of the heat source parameter is to increase the boundary layer as shown in fig. 4, which is as expected due to the fact that when heat is generated the buoyancy force increases which accelerates the flow rate and thereby giving rise to increase in the velocity profiles.

Fig. 3 has been plotted to depict the variation of temperature profiles against for different values of heat source parameter by fixing other physical parameters. From this graph we observe that temperature increase with increase in the heat source parameter because when heat is generated, the buoyancy force increases the temperature profiles. Figs. 5-6 display the effects of the chemical reaction parameter on the velocity and concentration profiles, respectively. As expected, the presence of the chemical reaction significantly affects the concentration profiles as well as the velocity profiles. It should be mentioned that the studied case is for a destructive chemical reaction. In fact, as chemical reaction increases, the considerable reduction in the velocity profiles is predicted, and the presence of the peak indicates that the maximum value of the velocity occurs in the body of the fluid close to the surface but not at the surface. Also, with an increase in the chemical reaction parameter, the concentration decreases. It is evident that the increase in the chemical reaction significantly alters the concentration boundary layer thickness but does not alter the momentum boundary layers.

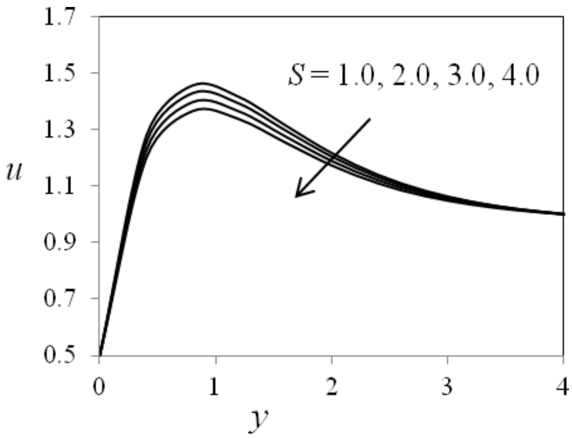

Figure 3. Velocity profiles for different values of Heat source parameter

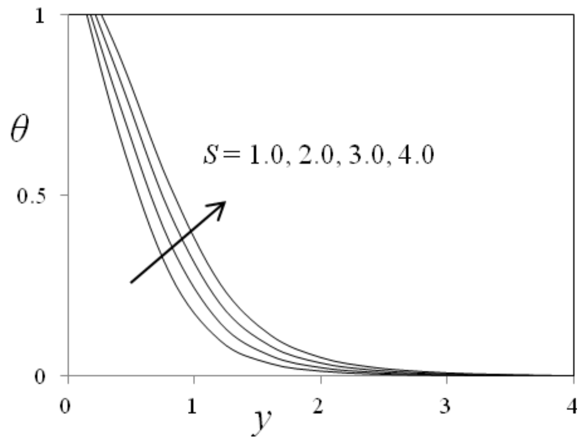

Figure 4. Temperature profiles for different values of Heat source parameter

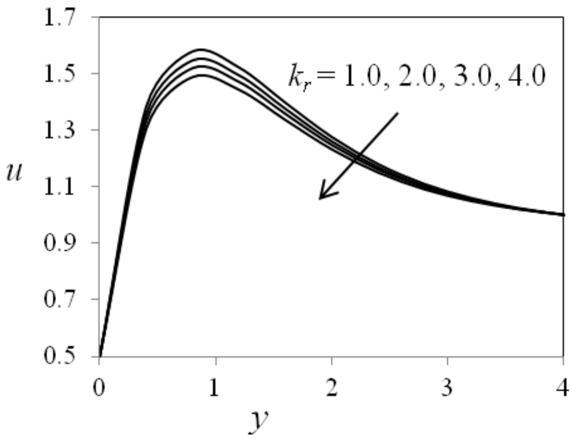

Figure 5. Velocity profiles for different values of Chemical reaction parameter

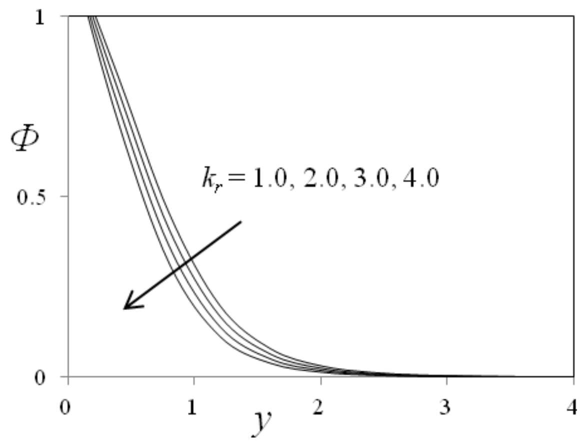

Figure 6. Concentration profiles for different values of Chemical reaction parameter

Fig. 7 illustrates the variation of velocity distribution across the boundary layer for several values of plate moving velocity in the direction of the fluid flow. Although we have different initial plate moving velocities, the velocity decrease to the constant values for given material parameters. The effects of Dufour and Soret numbers on velocity profiles are shown in the figs. 8-9 respectively. From these figures, we observed that increases in Soret and Dufour numbers lead to an increase in the fluid flow causes the momentum boundary layer thickness generally increases away from the plate satisfying the boundary conditions. From Fig. 10 as expected, the numerical results show that an increase in the Prandtl number (P_r) results a decrease of the thermal boundary layer and in general lower average temperature within the boundary layer. The reason is that smaller values of P_r are equivalent to increase in the thermal conductivity of the fluid and therefore heat is able to diffuse away from the heated surface more rapidly for higher values of P_r. Hence in the case of smaller Prandtl number the thermal boundary layer is thicker and the rate of heat transfer is reduced.

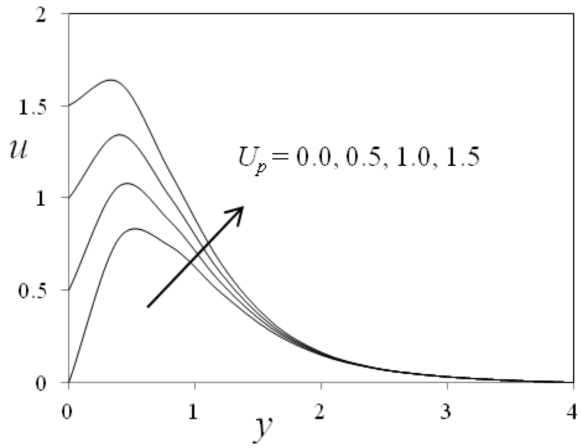

Figure 7. Velocity profiles for different values of Plate velocity

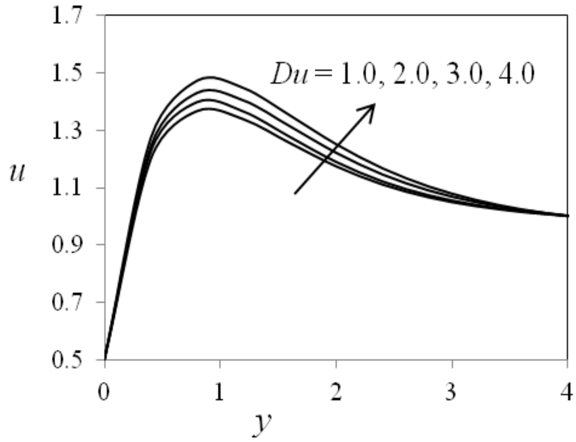

Figure 8. Velocity profiles for different values of Dufour number

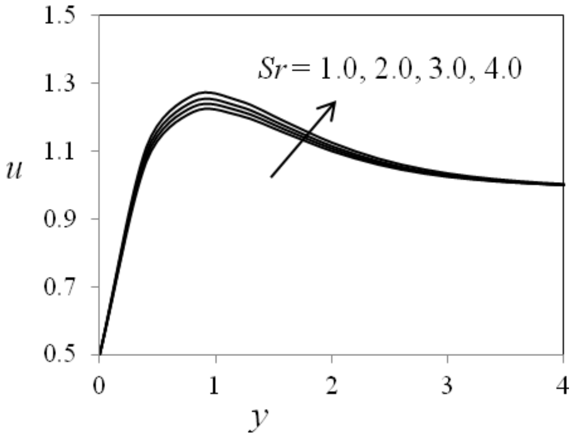

Figure 9. Velocity profiles for different values of Soret number

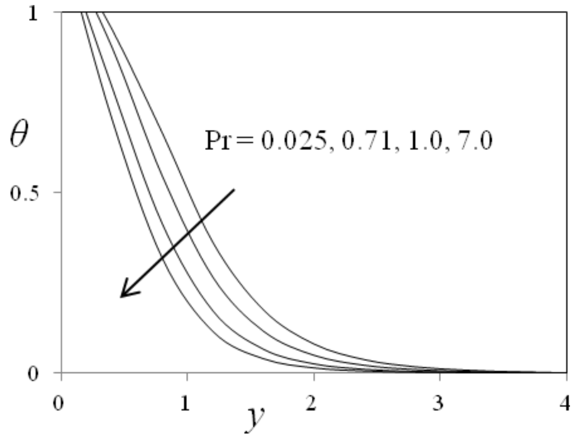

Figure 10. Temperature profiles for different values of Prandtl number

Fig. 11 shows the influence of Dufour number on fluid temperature. We observed an increase in the fluid temperature with an increase in the Dufour number. The effect of Schmidt number (*Sc*)on concentration profiles is shown in the fig. 12.

The Schmidt number characterizes the relative effectiveness of momentum and mass transport by diffusion, higher value of Sc Schmidt number lead to species diffusivity rate exceed the momentum diffusivity will diminish the concentration in the boundary layer. Fig. 13 demonstrates the effect of Soret number Sr on the species concentration boundary layer thickness when the remaining parameters are assumed to be fixed. From this figure we observed that, the concentration profiles are increasing with increasing values of Soret number.

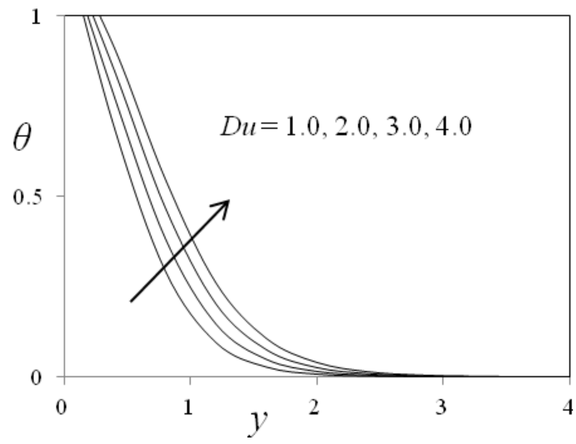

Figure 11. Temperature profiles for different values of Dufour number

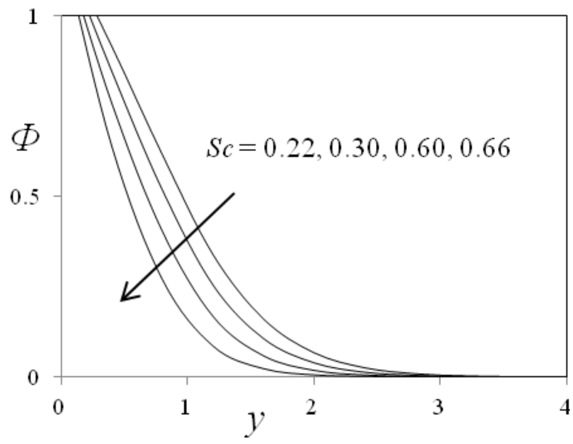

Figure 12. Concentration profiles for different values of Schmidt number

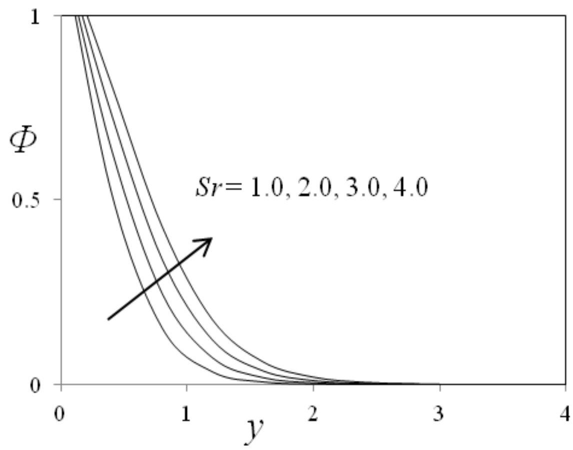

Figure 13. Concentration profiles for different values of Soret number

Table 1. Skin – friction results (τ) for the values of $G, G_c, P_r, S_c, K, S, S_r, D_u$ and k_r.

Gr	Gc	Pr	Sc	K	Sr	Du	S	k_r	τ
1.0	1.0	0.71	0.22	1.0	1.0	1.0	1.0	1.0	3.15875495
2.0	1.0	0.71	0.22	1.0	1.0	1.0	1.0	1.0	3.32655487
1.0	2.0	0.71	0.22	1.0	1.0	1.0	1.0	1.0	3.40582641
1.0	1.0	7.00	0.22	1.0	1.0	1.0	1.0	1.0	3.06234489
1.0	1.0	0.71	0.30	1.0	1.0	1.0	1.0	1.0	3.08339015
1.0	1.0	0.71	0.22	2.0	1.0	1.0	1.0	1.0	3.25661066
1.0	1.0	0.71	0.22	1.0	2.0	1.0	1.0	1.0	3.18062274
1.0	1.0	0.71	0.22	1.0	1.0	2.0	1.0	1.0	3.20641187
1.0	1.0	0.71	0.22	1.0	1.0	1.0	2.0	1.0	3.21600538
1.0	1.0	0.71	0.22	1.0	1.0	1.0	1.0	2.0	3.10806776

The profiles for skin – friction (τ) due to velocity under the effects of Grashof number, Modified Grashof number, Prandtl number, Schmidt number, Permeability parameter, Heat source parameter, Soret number, Dufour number and Chemical reaction parameter are presented in the table 1 respectively. We observe from this table, the skin – friction rises under the effects of Grashof number, Modified Grashof number, Soret number, Dufour number, Heat source parameter and Permeability parameter and falls under the effects of Prandtl number, Schmidt number and Chemical reaction parameter. The profiles for Nusselt number (Nu) due to temperature profile under the effect of Prandtl number, Dufour number and Heat source parameter are presented in the table – 2. From this table we observe that, the Nusselt number due to temperature profiles falls under the effects of Prandtl number and rises under the effect of Dufour number and Heat source parameter.

Table – 2: Rate of heat transfer (*Nu*) values for different values of Pr, Du and S.

Pr	*Du*	*S*	*Nu*
0.71	1.0	1.0	2.05942151
7.00	1.0	1.0	1.84629158
0.71	2.0	1.0	2.10654989
0.71	1.0	2.0	2.12456295

Table – 3: Rate of mass transfer (*Sh*) values for different values of Sc, Sr and k_r.

Sc	*Sr*	k_r	*Sh*
0.22	1.0	1.0	2.10548762
0.30	1.0	1.0	1.99548726
0.22	2.0	1.0	2.15486219
0.22	1.0	2.0	1.98269541

The profiles for Sherwood number (*Sh*) due to concentration profiles under the effect of Schmidt number, Soret number and Chemical reaction parameter are presented in the table 3. We see from this table the Sherwood number due to concentration profiles decreases under the effects of Schmidt number, Chemical reaction parameter and increases with increase of Soret number.

5. CONCLUSIONS

The governing equations for unsteady MHD convective heat and mass transfer flow past a semi – infinite vertical permeable moving plate embedded in a porous medium and the flow was subjected to a transverse magnetic field in presence of Soret and Dufour effects. The resulting partial differential equations were transformed into a set of ordinary differential equations solved by using finite difference method. Numerical evaluations of the numerical results were performed and graphical results were obtained to illustrate the details of the flow and heat and mass transfer characteristics and their dependence on some physical parameters.

1. An increasing Hartmann number, Chemical reaction parameter decreases the velocity of the flow field while increasing Permeability parameter, Soret number, Dufour number, Heat source parameter and Plate velocity is to increase the velocity of the flow field at all the points.
2. A growing Prandtl number decreases temperature and increases with increasing of Dufour number and Heat source parameter at all points of the flow field.
3. The Schmidt number and Chemical reaction parameter decreases the concentration and increases with increasing of Soret number at all points of the flow field.
4. An increasing Hartmann number, Prandtl number, Schmidt number and Chemical reaction parameter decreases the skin – friction coefficient.
5. An increasing Grashof number, Modified Grashof number, Permeability parameter, Soret number, Dufour number, Heat source parameter and Plate velocity is to increase the skin – friction coefficient.
6. A growing Prandtl number decreases Nusselt number and increases with increasing of Dufour number and Heat source parameter.

7. The Schmidt number and Chemical reaction parameter decreases Sherwood number and increases with increasing of Soret number.

REFERENCES

[1] Anghel, M., Takhar, H. S., Pop, I., *Studia universities – Bolyai, Mathematica*, **45**, 11, 2000.
[2] Emmunuel, O., Jonathan, S., Robert, H., *International Journal of Communications in Heat and Mass Transfer*, **35**, 908, 2008.
[3] Afify, A., *Applied Mathematical Modelling*, **31**, 1621, 2007.
[4] Lakshmi Narayana, P. A., Murthy, P. V. S. N., *Journal of Heat Transfer*, **130**, 104504, 2008.
[5] Postelnicu, A., *Heat and Mass Transfer*, **43**(6), 595, 2007.
[6] El – Arabawy, H. A. M., *Journal of Mathematics and Statistics*, **5**(3), 190, 2009.
[7] Postelnicu, A., *Heat and Mass Transfer*, **46**(8-9), 831, 2010.
[8] Tak, S. S., Mathur, R., Gehlot, R. K., *Thermal Science*, **14**(1), 137, 2010.
[9] Kesavaiah, D., Satyanarayana, Ch. P. V., Venkataramana, S., *International Journal of Applied Mathematics and Mechanics*, **7**(1), 52, 2011.
[10] Seddeek, M. A., Darwish, A. A., Abdelmeguid, M. S., *Communications in Nonlinear Science and Numerical Simulation*, **12**, 195, 2007.
[11] Das, U. N., Deka, R., Soundalgekar, V. M., *Journal of Forschung Im Ingenieurwesen – Engineering Research*, **60**, 284, 1994.
[12] Anjalidevi, S. P., Kandasamy, R., *Heat Mass transfer*, **35**, 465, 1999.
[13] Takhar, H. S., Chamhka, A. J., Nath, G., *International Journal of Engineering Science*, **38**, 1303, 2000.
[14] Muthucumaraswamy, R., *Forschung Im Ingenieurwesen*, **67**, 129, 2002.
[15] Afify, A., *Heat and Mass Transfer*, **40**, 495, 2004.
[16] Raptis, A., Perdikis, C., *International Journal of Non linear Mechanics*, 41, 527, 2006.
[17] Postelnicu, A., *Heat and Mass Transfer*, **43**(6), 595, 2007.
[18] Dulal Pal, Hiranmoy Mondal, *Nuclear Engineering and Design*, **256**, 350, 2013.
[19] Dulal Pal, Hiranmoy Mondal, *Journal of Magnetism and Magnetic Materials*, **331**, 250, 2013.
[20] Ching – Yang Cheng, *International Communications in Heat and Mass Transfer*, **38**(8), 1056, 2011.
[21] Dulal Pal, Hiranmoy Mondal, *Energy Conversion and Management*, **62**, 102, 2012.
[22] Srinivasa Raju, R., Sudhakar, K., Rangamma, M., *Journal of Institution of engineers*, **94**(2), 175, 2013.
[23] Dulal Pal, Sewli Chatterjee, *Applied Mathematics and Computation*, **219**(14), 7556, 2013.